LETTERS IN BIOMATHEMATICS
An International Journal

RESEARCH ARTICLE

OPEN ACCESS

A Non-Linear Host-Vector Mathematical Model for Vector-Borne Disease Transmission Under Seasonal Environmental Variability and Integrated Public Health Interventions

Memona[1*], **Tahniat Rehman**[2]

[1] Department of Biochemistry, University of Okara, Pakistan

[2] Department of Nutrition and Dietetics, The University of Faisalabad, Pakistan

ABSTRACT

The dynamics of vector-borne disease transmission track the interplay of environmental, ecological, demographic, and epidemiological factors at various temporal scales. This paper develops a non-linear host-vector compartmental system to describe the dynamics of transmission in the context of environmental seasonality and public health interventions. Human populations of susceptible, exposed, infected, and recovered groups are included in these compartments, as are vector populations of susceptible, exposed, and infected groups as well as larval and adult development phases. Personal protection, larvicides, and adulticides are included as intervention factors, and seasonality is introduced through the periodic transmission mechanism. Positivity, boundedness, feasibility, endemic and disease-free equilibria, threshold property, stability, and sensitivity analysis of the dynamical system's parameters are all examined in the mathematical model. While the Jacobian and Lyapunov approaches provide the qualitative description of the equilibria, the next-generation matrix provides a spectral threshold of the disease dynamics in terms of infection invasion. A numerical scale that links the intensity of interventions with the possibility for transmission is provided by the representation of the composite controls and the efficacy of interventions. In order to establish a mathematical basis for comprehending vector-borne transmission as a coupled biological dynamical system, the theory focuses on the interaction between non-linear transmission, seasonality, vector life cycle structure, and parameter reliance on interventions. In a high-dimensional state space, this theoretical method enables the quantitative examination of biological processes and intervention consequences.

ARTICLE HISTORY
Received September 27, 2026
Accepted October 31, 2026

KEYWORDS
Vector-Borne Disease Modeling,
Non-Linear Dynamical Systems,
Intervention Efficiency Index, Reproduction Number, Sensitivity Transmission Dynamics

1. Introduction

The dynamics of infectious disease transmission are significantly influenced by seasonality, with many pathogens displaying clear seasonal patterns. The changes in temperature, precipitation, and humidity brought on by climate change exacerbate the intricate relationships between parasites, hosts, and vectors (Swei et al., 2020). Vector-borne diseases (VBDs) have been around for a while and are now one of the biggest global public health issues, affecting millions of people annually and posing a serious danger to the security of global health. Currently, more than 50% of the world's population is at risk of catching VBDs, with both developed and developing nations being harmed (Padder et al., 2025). Mosquitoes are known vectors for some of the most widespread and fatal diseases, including malaria, dengue fever, chikungunya, Rift Valley fever, and yellow fever, among others (Padder et al., 2025). Therefore, mathematical epidemiology provides a useful method for

CONTACT Memona : memonashabbir45@gmail.com

characterizing biological phenomena in terms of differential equations and employing analytical techniques to investigate the existence of diseases, epidemic threshold values, and the effectiveness of interventions through reproduction numbers and stability theory (Erandi et al., 2021; Kamiya et al., 2020).

In recent years, tremendous progress in developing and improving mathematical models to better understand the dynamics of VBDs transmission. These models are critical instruments that enable for the research and analysis of the complicated interactions between vectors, diseases, and hosts (Padder & Khan, 2022). Some mathematical methods to comprehend the intricate dynamic behavior of biological issues, including infectious and non-communicable diseases, as well as the environmental factors that contribute to their spread. For example, models based on fractional calculus, bifurcation analysis, and differential equations have been developed to offer greater insights into the mechanisms driving disease progression and control techniques (Momoh et al., 2024). The state will be able to create policies and restrict the spread of disease with aid of the prediction made using a mathematical model. Additionally, model offers conceptual conclusions for the dynamics of disease transmission, including thresholds, basic reproduction numbers, contact numbers, and replacement numbers (Prasad et al., 2022).

It has long been known that mathematical models are useful tools for comprehending the dynamics of infectious diseases and creating successful intervention plans. Traditional compartmental models, such the Susceptible-Infected-Recovered (SIR) and Susceptible-Exposed-Infectious-Recovered (SEIR) frameworks, study the dynamics of disease transmission using ordinary differential equation systems, where state variables are defined in terms of epidemiological compartments and interactions. Because SEIR-type models specifically include an exposed class to represent the incubation time prior to infectiousness, they are particularly suitable for diseases exhibiting a latent period (Mubarak et al., 2026). The standard compartmental models may include age structure, delay, or spatial dynamics to represent more intricate real-world behavior (Dhandapani et al., 2026). By adding memory kernels or a delay in state dependency, these models modify the dynamical system. However, these models sometimes exclude certain stages of the vector lifespan or fail to account for the combined effects of many control strategies. The unique ecological and socioeconomic factors that influence the spread of disease are rarely taken into account in models (Alalhareth et al., 2023). Non-linear threshold phenomena, multistability, infection persistence or extinction, and instability dependent on parameter changes are some of the characteristics that these systems may exhibit. The spectral radius of the next-generation matrix or operator is typically used to determine the amount R_0 for deterministic compartmental models, resulting in a bifurcation threshold for infection invasion and extinction. The mathematical relationship between the two ideas is seen in the spectrum of the Jacobian assessed at the disease-free equilibrium point.

This work mathematically addresses the previously described shortcomings of previous models by developing a novel host-vector model that takes into consideration the seasonal change of the environment, the mosquito life cycle, and many intervention tactics in a single deterministic model. The current study addresses this by creating a deterministic non-linear host-vector compartmental model in which the human population is divided into susceptible, exposed, infected, and recovered classes, and the vector population is divided into susceptible, exposed, and infected classes, in addition to mosquito larval and adult stages. In this model, personal protection, larvicides, and adulticides are taken into consideration through the application of controls, and the periodicity of the environment is addressed by incorporating a periodically fluctuating transmission rate. The mathematical analysis focuses on the qualitative aspects of the system, such as the solutions' positivity and boundedness, the creation of a positive invariant feasible region, the identification of endemic and disease-free equilibria, the computation of the basic reproduction number using the next generation matrix method, and stability analysis using Jacobian linearization and Lyapunov functions. Finally, a Composite Control Function and an Intervention Efficiency Index are created to quantify how the intervention's intensity affects transmission capacity.

2. Research Objective of Study

The objective of this study is to create and examine a mathematical non-linear compartmental model that takes into account the growth of mosquitoes as well as the concerted efforts of public health interventions in the seasonally forced transmission of disease by mosquitoes. This study uses a composite control formulation and efficiency measurement to quantify the impact of intervention intensity on transmission potential while examining the dynamic properties, equilibrium configurations, reproductive thresholds, stability, and parameter sensitivities of the model.

3. Literature Review

Recent advances in the study of host-vector epidemics have examined the issue of disease transmission in terms of a differential equation-described non-linear dynamical system. The equilibrium structure, thresholds,

bifurcations, and stability that underpin a disease's presence or eradication have received more attention. In particular, contemporary research has focused on modeling frameworks that are oriented towards control, backwards bifurcation, and complex dynamic behaviors in vector-borne disease systems. These investigations highlight the importance of dynamical consistency and comprehensive threshold assessments for understanding long-term disease persistence and the effectiveness of control measures (Rivu et al., 2025). Studies have used time-dependent transmission parameters and periodically forced non-autonomous models to examine the effects of seasonality and temporal variations in contact rates on the dynamics of infectious diseases. The governing differential equations in such models incorporate temporal dependency (Kronfeld-Schor et al., 2021; Swei et al., 2020). Recent research has focused on modelling frameworks for the control-oriented, backwards bifurcation, and complex dynamics of vector-borne disease systems, emphasizing the importance of dynamical consistency and threshold evaluations in investigating disease persistence and control measure efficacy (Bera et al., 2023). The existing research clearly shows that the combination of various control strategies, such as larvicides and adulticides, has a considerable impact on the fundamental reproduction number and stability of disease-free and endemic equilibria (Padder et al., 2025). Research highlights that Yan et al. (2025) found seasonality has a significant influence on emergence probability and extinction threshold in epidemic models when it affects disease transmission, recovery, and vector births or deaths, with the peak of emergence occurring before the peak of seasonality. According to their findings, there can be paradoxical behavior in seasonally variable settings, which can lead to a reduced emergence likelihood compared to constant conditions. Furthermore, Akanni (2026) supports these findings by showing that seasonal mosquito recruitment increases epidemic peaks at times of high vector abundance. The study by Jothika and Radhakrishnan (2025) looks at a vector-host model with time delays and saturated treatment functions. It demonstrates how treatment delays have a significant impact on the dynamics of the disease and that both the endemic and disease-free equilibria can be stable depending on the value of the basic reproduction number. Research demonstrated that the work conducted by Romero-Leiton et al. (2025) future research on Zika virus modeling must consider data robustness and validation using various data source. Study claimed that Fesce et al. (2025) employ deterministic compartmental models to assess the efficacy of interventions for West Nile virus transmission, demonstrating that vector-based interventions particularly larviciding and breeding site reduction are more effective than host-based therapies. The efficiency of all the interventions is time-dependent, peaking in midsummer, which also highlights the need of mathematical modelling in developing an effective intervention approach given restricted resources. Research claims that through the use of the reproduction number R_0, Cui et al. (2025) developed a degenerate reaction-diffusion model that demonstrated how seasonality and heterogeneity impact mosquito population dynamics and established threshold conditions for mosquito population extinction or persistence. Manisha and Kumar (2025) demonstrated that the best cost-effective method of reducing disease incidence is to combine information-induced self-protection with pesticide usage in a compartmental model and use Pontryagin's Maximum Principle. Studies claimed that fractional modelling has been utilized to incorporate memory into models of vector-borne diseases by employing sensitivity analysis to validate the impact of vaccination using Caputo fractional derivative to determine the stability criterion. Thus, it may be said that complex techniques are required to simulate the dynamics of vector-borne diseases (Ullah et al., 2026). This study offers a unified non-linear dynamical model for host-vector interactions in which the transmission mechanism incorporates several control measures and seasonality. The theoretical methodology includes a positive invariant dynamical system, normalized sensitivity analysis of parameters, stability analysis based on Jacobian and Lyapunov techniques, and threshold determination using the next-generation matrix method. In order to guaranty that solutions, remain inside a realistic biological region, mathematical epidemiological models also require positivity and boundedness of solutions. In order to connect mathematical formulation with biological interpretation, positively invariant sets are importan.

4. Research Methodology

4.1 Development of Mathematical Model

The SEIR model is a compartmental epidemiological model used to analyze and forecast the spread of infectious diseases within a community. A general transfer diagram for the SEIR model is schematically shown in Figure 1. Because it takes into consideration the latent period more especially, the exposed class which models like SIR or SIS do not, this model is preferred above others. It also keeps things simpler than devices with many sections. The model assumes homogeneous mixing, deterministic transmission dynamics, non-negative state variables, solutions that are continuously differentiable and biologically feasible parameter values.

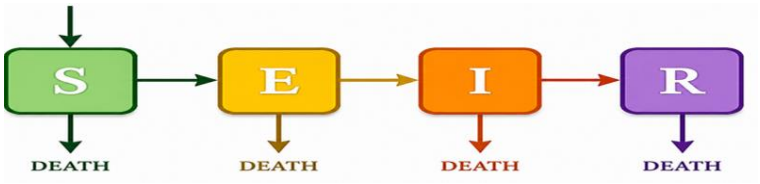


Figure 1: Compartmental Transfer Diagram of SEIR Model

4.1.1 Model Framework

The host and vector populations into separate epidemiological groups using a compartmental mathematical model was employed. In addition to explicitly stated larva and adult mosquito compartments, the model takes into account human (susceptible, exposed, infected, and recovered) and vector (susceptible, exposed, and infectious) compartments.

$$X(t) = (S_h, E_h, I_h, R_h, S_v, E_v, I_v, L, A)^T \quad (1)$$

with $X(t)\ \epsilon\ R_+^9$ representing the vector demographic process and epidemiological states at time t. Four subclasses comprise the whole human population at time t, represented by $N_h(t)$: susceptible humans $S_h(t)$, exposed humans $E_h(t)$, infectious humans $I_h(t)$, and recovered humans $R_h(t)$.

$$N_h(t) = S_h(t) + E_h(t) + I_h(t) + R_h(t) \quad (2)$$

The total vector population at time t, denoted by $N_v(t)$, is partitioned into susceptible vectors $S_v(t)$, exposed vectors $E_v(t)$, infectious vectors $I_v(t)$, larvae $L(t)$, and adult mosquitoes $A(t)$, so that,

$$N_v(t) = S_v(t) + E_v(t) + I_v(t) + L(t) + A(t) \quad (3)$$

The force of infection in the human population is decreased by a factor $(1 - u_1)$, where u_1 is a measure of personal protection, including behavioral interventions, protective gear, and repellents. The variables in control, larvicidal and adulticidal control measures' strengths are denoted by u_2 and u_3, respectively. The death rate of adult vectors is increased in proportion to r_0 by adulticidal action. The resulting non-linear system of nine ordinary differential equations is given by

$$\frac{dS_h}{dt} = b_1 + cN_h - \beta_1(1-u_1)S_hI_v - \mu_hS_h \quad (4)$$

$$\frac{dE_h}{dt} = \beta_1(1-u_1)S_hI_v - (\alpha_h + \mu_h)E_h \quad (5)$$

$$\frac{dI_h}{dt} = \alpha_hE_h - (\gamma_h + \mu_h + \delta_h)I_h \quad (6)$$

$$\frac{dR_h}{dt} = \gamma_hI_h - \mu_hR_h \quad (7)$$

$$\frac{dS_v}{dt} = b_3 + b_2A - \beta_2S_vI_h - (\mu_v + r_0\mu_3)S_v \quad (8)$$

$$\frac{dE_v}{dt} = \beta_2S_vI_h - (\mu_v + r_0\mu_3 + \alpha_v)E_v \quad (9)$$

$$\frac{dI_v}{dt} = \alpha_vE_vI_h - (\mu_v + \delta_v + r_0\mu_3)I_v \quad (10)$$

$$\frac{dL}{dt} = pA - (q + \mu_2 + d_L)L \quad (11)$$

$$\frac{dA}{dt} = qL - (\mu_3 + d_A)A \quad (12)$$

Incorporating these assumptions, the model is schematically illustrated in Figure 2.

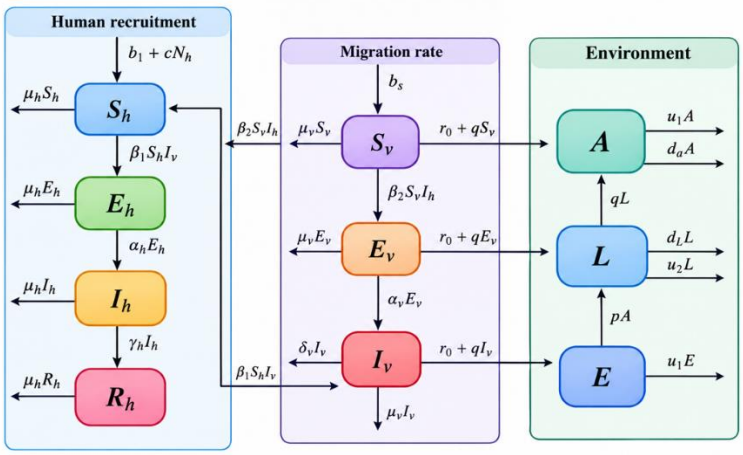


Figure 2: Flow Chart of the Modified SEIR Model Showing the Interaction and Transfer Between Different Classes of the Human and Vector

4.1.2 Mathematical Formulation of the Integrated Control Framework

The novel approach presented here modifies the deterministic host-vector SEIR model by incorporating a mathematically coupled multi-scale transmission process that incorporates mosquito development phases, environmental forces, and multiple control strategies within a unified non-linear dynamic system. The vector-borne disease modelling methodologies used in this study differ from those used previously in that the former use a periodic transmission function.

$$\beta_h(t) = \beta_{h0}(1 + \varepsilon \cos\left(\frac{2\pi t}{T}\right)) \tag{13}$$

where $0 \leq \varepsilon < 1$ corresponds to seasonality strength, and T represents the environmental period. The seasonally driven model is a non-autonomous non-linear dynamical system since $\beta_h(t)$ is explicitly a function of t. Thus, the compact version of the seasonally varying model is as follows:

$$\frac{dX}{dt} = F(t, X, \theta) \tag{14}$$

With,

$$F(t + T, X, \theta) = F(t, X, \theta \tag{15}$$

T stands for the forcing duration in this case. The vector field's temporal periodicity is evident. As a result, the system makes it possible to analyze the periodic and transitory dynamics of disease transmission under seasonality. The corresponding autonomous system without the impact of seasonality is considered in the equilibrium analysis and threshold analysis (setting $\varepsilon = 0$). The transmission dynamics are then numerically analyzed using the entire periodic system. This method aids in distinguishing the equilibrium-based stability characteristics from the dynamics' seasonality.

Thus, the power of infection is

$$\lambda_h(t) = \frac{(1-u_p)\beta_h(t)I_v}{N_h} \tag{16}$$

which uses mathematics to integrate seasonal fluctuation and behavioral intervention. Furthermore, the intervention strategy is captured in a combined control function.

$$\theta(u_p, u_p, u_p) = (1 - u_p)(1 - u_l)(1 - u_a) \tag{17}$$

This allows a joint assessment of personal protection, larvicides, and adulticides using one unified mathematical model. Thus, the reproduction number takes the form of

$$R_e = \theta(u_p, u_p, u_p)R_0 \tag{18}$$

This provides a concise mathematical relationship between intervention effort and disease persistence. Methodologically, this methodology produces a broad non-linear host-vector dynamical system with a positively invariant feasible region, threshold-type dynamics based on R_e, Lyapunov-type requirements for global stability,

and parameter sensitivity analysis. This proposed modelling approach thus provides a mathematically solid analytical approach for assessing the combined influence of seasonality and intervention efforts on vector-borne disease spread.

4.2 Model Parameters

For the model to be epidemiologically meaningful, all state variables must remain non-negative, the non-negative orthant is mathematically equivalent to the acceptable state space.

$$R_+^9 = (X \epsilon R^9 : X_i \geq 0, i = 1, \dots, 9) \tag{19}$$

Thus, the subset of R_+^9 for which the following is true describes the biologically plausible state space. It is assumed that every parameter is biologically significant and non-negative. Table 1 and 2 provide the primary parameters.

Table 1: Nomenclature of Various Parameters Involved in the Model

Parameters	Description
b_1	Recruitment rate of the human population
c	Per-capita demographic growth contribution
β_1	Transmission rate from infectious vectors to susceptible humans
α_h	Transmission rate from infectious humans to susceptible vectors
γ_h	Progression rate from exposed to infectious humans
δ_h	Recovery rate of infectious humans
μ_h	Disease-induced mortality rate in humans
b_3	Natural mortality rate of humans
b_2	Recruitment of susceptible vectors by migration
b_1	Recruitment of susceptible vectors from adult mosquitoes

Table 2: Nomenclature of Various Parameters Involved in the Model

Parameters	Description
μ_v	Natural mortality rate of vectors
δ_v	Disease-induced mortality rate in vectors
α_v	Progression rate from exposed to infectious vectors
p	Oviposition rate contributing to larval recruitment
q	Maturation rate from larvae to adult mosquitoes
d_L	Natural mortality rates of larvae
d_A	Natural mortality rates of adult mosquitoes
r_0	Proportional increase in adult mosquito mortality due to control
u_1	Control parameter representing personal protection
u_2	Control parameter representing larvicidal intervention
u_3	Control parameter representing adulticidal intervention

$$S_h(0) > 0, E_h(0) \geq 0, I_h(0) \geq 0, R_h(0) \geq 0, S_v(0) > 0,\ E_v(0) \geq 0,\ I_v(0) \geq 0, L(0) \geq 0, A(0) \geq 0 \tag{20}$$

To guarantee the epidemiological viability of disease transmission dynamics, assume strictly positive starting susceptible human $S_h(0)$ and vector populations $S_v(0)$. It is expected that every other state variable is non-negative. Hence, the feasible region,

$$\Omega = (X \epsilon R_+^9 : N_h \leq N_h^{max}, N_v \leq N_v^{max}) \tag{21}$$

is positively invariant, meaning

$$X(0) \epsilon \Omega \Longrightarrow X(t) \epsilon \Omega, t \geq 0 \tag{22}$$

As a result, every trajectory that begins with an initial condition that has biological significance will be positive and bounded for all subsequent time. The model is locally Lipschitz in X since its right-hand side is continuously differentiable with respect to the state variables given biological parameter values. This suggests that the starting-value problem has a unique solution for any biological initial value $X(0) \epsilon \Omega$. This creates a distinct biologically significant trajectory for $t \geq 0$ when combined with the boundedness of the feasible set. For any $t > 0$, standard comparison arguments ensure that the solutions of systems (3 – 11) remain non-negative.

4.3 Total Human and Vector Population Dynamics

By summarizing the equations (4 – 7), it yields,

$$\frac{dN_h}{dt} = b_1 + (c - \mu_h)N_h - \delta_h I_h \tag{23}$$

So, $\delta_h I_h \geq 0$, it is obtained that

$$\frac{dN_h}{dt} \leq b_1 - (c - \mu_h)N_h \tag{24}$$

For any $t > 0$, the human population stays bounded and positive as long as $\mu_h > c$. For vector population dynamics, with the help of equations (8 – 12),

$$\frac{dN_v}{dt} = b_3 + b_3 A - (\mu_v + r_0\mu_3)(S_v + E_v) - (\mu_v + \delta_v + r_0\mu_3)I_v - (u_2 + d_L)L - (u_3 + d_A)A \tag{25}$$

The vector subsystem maintains mass balance consistency because all internal transitions infection, progression, oviposition, and maturation cancel out upon summation. Using $S_v + E_v + I_v + L + A = N_v$, we obtained,

$$\frac{dN_v}{dt} \leq b_3 + b_2 N_v - \emptyset N_v \tag{26}$$

If $\phi > b_2$, then $N_v(t)$ remains bounded for all $t > 0$ by standard comparison arguments. Proposition 1. If $(S_h, E_h, I_h, R_h, S_v, E_v, L, A)$ is a solution of equations (4 – 12) with initial conditions (20), then the region,

$$\Omega = [R_+^9 : N_h \leq \frac{b_1}{\mu_h - c}, N_v \leq M_v] \tag{27}$$

The overall human and vector populations are still bounded and non-negative according to equations (20) and (7). Trajectories beginning in Ω cannot exit Ω because every equation in (4 – 12) maintains non-negativity. As a result, Ω is attractive and positively invariant.

4.4 Disease Free Equilibrium

The condition in which there is no ongoing infection in either the human or vector populations is known as the disease-free equilibrium (DFE). Therefore, at the DFE we imposed

$$E_h = I_h = R_h = 0, \; E_v = I_v = 0 \tag{28}$$

In these circumstances, the vulnerable human and vector populations, as well as the larval and adult phases, are governed by the following subsystem of system (4 – 12):

$$\frac{dS_h}{dt} = b_1 + cN_h - \mu_h S_h \tag{29}$$

$$\frac{dS_v}{dt} = b_3 + b_2 A - (\mu_v + r_0\mu_3)S_v \tag{30}$$

$$\frac{dL}{dt} = pA - (q + u_2 + d_L)L \tag{31}$$

$$\frac{dA}{dt} = qL - (u_3 + d_A)A \tag{32}$$

4.4.1 Human Component and Vector Larval-Adult Subsystem

As, $N_h = S_h$ at disease free equilibrium, human equation becomes,

$$\frac{dS_h}{dt} = b_1 + cS_h - \mu_h S_h \tag{33}$$

and by setting $\frac{dS_h}{dt} = 0$, yields,

$$S_h^0 = \frac{b_1}{\mu_h - c} \tag{34}$$

offered $\mu_h > c$, guaranteeing biological viability and positivity.
The steady-state equations for vector L and A are,

$$pA_0 = (q + u_2 + d_L)L_0, \; qL_0 = (u_3 + d_A)A_0 \tag{35}$$

By solving this linear system, it gives,

$$A_0 = \frac{pq}{(q + u_2 + d_L)(u_3 + d_A)}A_0 \tag{36}$$

Thus, a non-trivial solution exists if and only if,

$$pq = (q + u_2 + d_L)(u_3 + d_A) \tag{37}$$

If not, the trivial solution $L_0 = A_0 = 0$ is found. The aforementioned relations uniquely determine the positive equilibrium values in the physiologically relevant scenario where adult mosquitoes persist.

4.4.2 Susceptible Vector Component

At the steady state,

$$S_v^0 = \frac{b_3 + b_2 A_0}{\mu_v + r_0 \mu_3} \tag{38}$$

Consequently, the disease-free equilibrium is given by $E_1 = S_h^0, 0, 0, 0, S_v^0, 0, 0, L_0, A_0$, where the definitions of S_h^0, S_v^0, L_0, and A_0 are given above. There is no circular dependence because each equilibrium component is specifically determined by the system characteristics.

4.5 Reproduction Number

We used the next-generation matrix method created in order to calculate the basic reproduction number R_0. The equations (4 – 12)'s infected compartments are identified as (E_h, I_h, E_v, I_v). Let V be the vector of leftover transition terms and F be the vector of fresh infection terms. The matrices are obtained by linearizing the infected subsystem around the disease-free equilibrium E_1.

$$F = \begin{pmatrix} 0 & 0 & 0 & \beta_1(1-u_1)S_h^0 \\ 0 & 0 & 0 & 0 \\ 0 & \beta_2 S_v^0 & 0 & 0 \\ 0 & 0 & 0 & 0 \end{pmatrix} \tag{39}$$

$$V = \begin{pmatrix} \alpha_h + \mu_h & 0 & 0 & 0 \\ -\alpha_h & \gamma_h + \mu_h + \delta_h & 0 & 0 \\ 0 & 0 & \alpha_v + \mu_v + r_o u_3 & 0 \\ 0 & 0 & 0 & \mu_v + \delta_v + r_o u_3 \end{pmatrix} \tag{40}$$

The basic reproduction number is defined as the spectral radius of FV^{-1}:

$$R_0 = \rho(FV^{-1}) \tag{41}$$

A direct computation yields,

$$R_0 = \sqrt{\frac{\beta_1 \beta_2 (1-u_1) \alpha_h \alpha_v S_v^0 S_h^0}{(\alpha_h + \alpha_v)(\gamma_h + \mu_h + \delta_h)(\alpha_v + \mu_v + r_o u_3)(\mu_v + \delta_v + r_o u_3)}} \tag{42}$$

The two-step transmission mechanism between host and vector populations is reflected in the square root structure. In terms of biology, R_0 is the anticipated number of secondary human infections that result from a single sick person being introduced into a population that is completely susceptible through host-vector interaction.

4.5.1 Endemic Equilibrium

The endemic equilibrium relates to a steady condition in which infection persists in both the human and vector populations. When equations (4 – 12) reach equilibrium, we supposed that all time derivatives are equal to zero i.e. $E_h^* > 0$, $I_h^* > 0$, $E_v^* > 0$, $I_v^* > 0$. From the human and vector subsystem at steady state, we obtained,

$$E_h^* = \frac{\beta_1(1-u_1) S_h^* I_v^*}{\alpha_h + \mu_h}, \; I_h^* = \frac{\alpha_h E_h^*}{\gamma_h + \delta_h + \mu_h} \tag{43}$$

$$E_v^* = \frac{\beta_2 S_h^* I_v^*}{\alpha_v + \mu_v + r_o u_3}, \; I_v^* = \frac{\alpha_h E_h^*}{\mu_v + \delta_v + r_o u_3} \tag{44}$$

A consistency criterion connecting infected compartments is obtained by recursively substituting these relations. Simplified, this condition becomes $R_0^2 = 1$.

Therefore, a positive endemic equilibrium exists if and only if $R_0 > 1$. The disease-free equilibrium is the only biologically possible equilibrium where $R_0 \leq 1$. The algebraic steady-state relations above uniquely identify the infected compartments after $R_0 > 1$, and the balancing equations (4 – 12) yield the remaining susceptible and vector-stage components. The endemic equilibrium is unique in Ω and has biological significance since all parameters are positive and the feasible region Ω is invariant.

4.6 Stability Analysis of Model Equilibrium

The local and global stability characteristics of the endemic and disease-free equilibria of equations (4 – 12) are examined in this section. The analysis adheres to traditional reasoning in compartmental epidemic modelling and non-linear dynamical systems.

4.6.1 Local Stability Analysis of Disease Free Equilibrium

If $R_0 < 1$, the disease-free equilibrium E_1 is locally asymptotically stable; if $R_0 > 1$, it is unstable. A Jacobian matrix with a block structure dividing infected and uninfected compartments is produced by linearizing equations (4 – 12) about the disease-free equilibrium E_1. Under biologically plausible parameter settings, the uninfected subsystem's eigenvalues are strictly negative. The infected subsystem, whose linearization aligns with the next-generation matrix formulation utilized in the derivation of R_0, thereby determines the stability of E_1. Every time $R_0 < 1$, E_1 is locally asymptotically stable. On the other hand, E_1 loses stability and the dominating eigenvalue turns positive if $R_0 > 1$.

4.6.2 Local Stability Analysis of Endemic Equilibrium

If $R_0 > 1$, the equations (4 – 12) admits a singular physiologically viable endemic equilibrium E_2, which is locally asymptotically stable in the feasible area Ω. Specifically, if and only if $R_0 > 1$, the infected components $(E_h^*, I_h^*, E_v^*, I_v^*)$ are positive, guaranteeing biological viability. To determine local stability, we linearize system (4 – 12) about E_2 and compute the Jacobian matrix $J(E_2)$. Since E_2 sits in the interior of Ω, all equilibrium components are positive.

The characteristic polynomial of $J(E_2)$ can be written in block form to differentiate between the epidemiological and demographic subsystems. As a result, the endemic equilibrium E_2 is locally asymptotically stable and all of the eigenvalues of $J(E_2)$ have negative real portions.

4.6.3 Global Stability Analysis of Disease Free Equilibrium

The disease-free equilibrium E_1 is globally asymptotically stable in Ω whenever $R_0 \leq 1$. Consider the Lyapunov function,

$$V = E_h + \frac{Q_1}{\alpha_h} I_h + E_v + \frac{Q_7}{\alpha_v} I_v \tag{45}$$

where $Q_1 = \alpha_h + \mu_h$ and $Q_7 = \alpha_v + \mu_v + r_o u_3$. This function only disappears in the disease-free equilibrium and is non-negative in Ω. Differentiating V along system (4 – 12) solutions and replacing the infected subsystem equations results in,

$$\frac{dV}{dt} \leq (R_0 - 1)\theta \tag{46}$$

where θ is a function of the infected variables that is not negative. Therefore, if $R_0 < 1$, we get $\frac{dV}{dt} \leq 0$, and equality only holds when every infected compartment disappears.

4.6.4 Global Stability Analysis of Endemic Equilibrium

As long as there is no backwards bifurcation, the endemic equilibrium E_2 is globally asymptotically stable in Ω if $R_0 > 1$. A unique positive equilibrium E_2 exists when $R_0 > 1$, making the disease-free equilibrium unstable. Examine a Volterra-type Lyapunov function with its center at E_2:

$$W = \sum_i (x_i - x_i^* - x_i^* \ln \frac{x_i}{x_i^*} \tag{47}$$

where x_i denotes each epidemiological state variable. Only at E_2 does the non-negative function W disappear. Differentiating W along equations (4 – 12) trajectories and applying the steady-state relations fulfilled at E_2 results in $\frac{dV}{dt} \leq 0$.Only in the endemic equilibrium does equality hold.

4.7 Sensitivity Analysis of Reproduction Number

We calculated the normalized forward sensitivity index of R_0 with regard to each parameter p in order to assess the relative significance of model parameters on disease transmission, as described by

$$\gamma_p^{R_0} = \frac{\partial R_0}{\partial p} \times \frac{p}{R_0} \tag{48}$$

The relative change in R_0 caused by a relative change in parameter p is measured by this index. With R_0's clear expression, it obtained

$$\gamma_{\beta_1}^{R_0} = \frac{1}{2},\ \gamma_{\beta_2}^{R_0} = \frac{1}{2} \tag{49}$$

suggesting that the greatest beneficial impact on the spread of disease comes from the rates of transfer from vector to host and host to vector. As,

$$\gamma_{u_1}^{R_0} = -\frac{1}{2} \times \frac{u_1}{1-u_1} \tag{50}$$

demonstrating that R_0 is much decreased when personal protection is increased. The efficacy of adulticidal measures is confirmed by negative sensitivity indices for parameters related to vector mortality, such as μ_v and r_0.

4.8 Intervention Efficiency Index

To measure the success of the integrated intervention, we defined the index of intervention efficiency using the following formula:

$$\varepsilon = \frac{R_0 - R_e}{R_0},\ 0 \le \varepsilon \le 1 \tag{51}$$

where R_0 is the basic reproduction number in the absence of any intervention and R_e is the effective reproduction number when interventions are present. The indicator represents the proportion of disease spread decrease achieved through a mix of therapies. An intervention strategy is considered effective whenever $\varepsilon > 0$, while $\varepsilon \to 1$, indicates near-complete suppression of disease transmission. Conversely, $\varepsilon \approx 0$, suggests that the adopted control policies have a negligible impact on epidemic processes. When opposed to the traditional threshold technique, which relies just on the reproduction number, the mathematical parameter provides an additional quantitative measure for evaluating the effectiveness of integrated intervention policies.

5. Results

5.1 Analysis of Composite Control Function with Reproduction Number and Intervention Effective Index

The mathematical relationship between the Composite Control Function, the Intervention Efficiency Index, and the Effective Reproduction Number is shown in Table 3. This information provides a theoretical framework for determining the effects of increased intervention levels on transmission dynamics and epidemic thresholds.

Table 3: The Mathematical Influence of Integrated Intervention Intensity on Disease Dynamics is Represented by a Numerical Link Between the Composite Equilibrium Control Function (θ), Suggested Intervention Efficiency Index (ϵ), and Effective Reproduction Number R_e

Composite Control Function (θ)	Intervention Efficiency Index (ε)	Effective Reproduction Number (R_e)	Composite Control Function (θ)	Intervention Efficiency Index (ε)	Effective Reproduction Number (R_e)
1	0.0	2.50	0.45	0.55	1.125
0.95	0.05	2.375	0.40	0.60	1.0
0.90	0.10	2.25	0.35	0.65	0.875
0.85	0.15	2.125	0.30	0.70	0.75
0.80	0.20	2.0	0.25	0.75	0.625
0.75	0.25	1.875	0.20	0.80	0.50
0.70	0.30	1.75	0.15	0.85	0.375
0.65	0.35	1.625	0.10	0.90	0.25
0.60	0.40	1.50	0.05	0.95	0.125
0.55	0.45	1.375	0.0	1.00	0
0.50	0.50	1.25			

Figure 3(a) illustrates the mathematical relationship between the Composite Control Function (θ) and the recommended Intervention Efficiency Index (ϵ). As the value of the composite control function decreases from 1 to 0, indicating that integrated interventions are being used more efficiently, the intervention efficiency index increases linearly from 0 to 1. The linear relationship demonstrates that improved implementation of personal protection, larvicidal control, and adulticidal control results in greater disease control efficiency. The suggested index's linear properties allow for the assessment of intervention efficiency and demonstrate that maximum efficiency can be achieved by using interventions optimally.

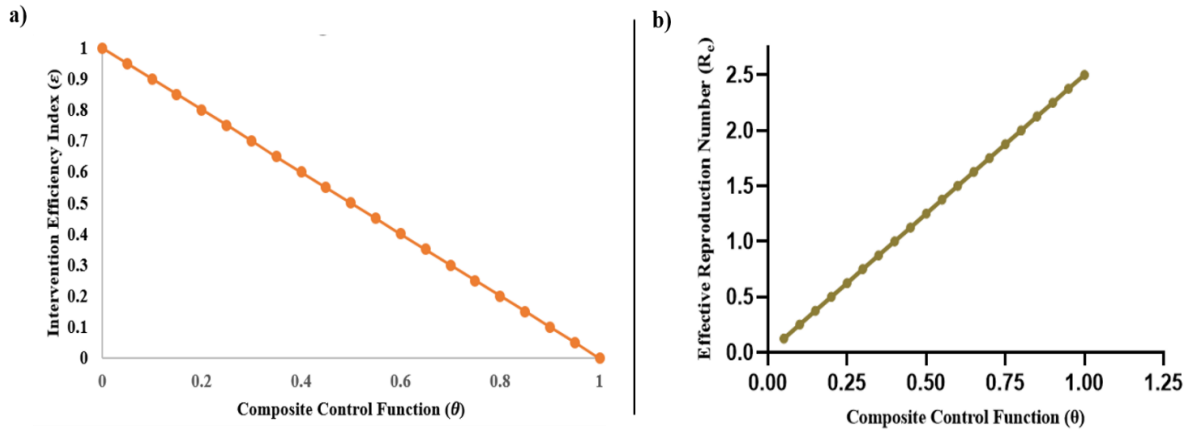


Figure 3: a) Connection Between the Suggested Intervention Efficiency Index (ϵ) and Composite Control Function (θ), b) Connection Between the Effective Reproduction Number (R_e) and Composite Control Function (θ) Demonstrates How More Successful Treatments Lower Epidemic Threshold and the Transmission Potential Figure 3(b) Shows the Correlation Between the Composite Control Function (θ) and the Effective Reproduction Number (R_e)

The results reveal that increasing the intensity of interventions causes a constant decline in the value of the effective reproduction number due to the disease's reduced ability to propagate across the host-parasite system. The pandemic threshold occurs when $R_e = 1$, after then, disease maintenance is no longer feasible. The mathematical relationship indicates that the analytical relation $R_e = \theta R_0$ holds true, demonstrating the effectiveness of public health efforts.

5.2 Numerical Interpretation of Compartmental Model

While retaining the biological significance of recruitment, transmission, progression, recovery, vector mortality, seasonality, and the three controls, a parameter setting was established independently of any prior data set reported in the study. The data set produced by the model is intended to be utilized as a simulation set.

Table 4: Seasonal Host-Vector Simulation Model's Baseline Parameters

State Variable	Initial Value	State Variable	Initial Value
$S_h(0)$	1200	$R_v(0)$	310
$E_h(0)$	12	$E_v(0)$	5
$I_h(0)$	6	$I_v(0)$	1.5
$R_h(0)$	0	$L(0)$	140
$A(0)$	70		

Figure 4 depicts the development of the numerical solution of the nine-state variable for the seasonally forced non-linear system with control. Without unbounded oscillations, the human compartment gradually shifts from the vulnerable to the exposed, infected, and recovered phases. The human population's infection rate rises from its starting point to a maximum of 12.5. Due to the combined effects of larvicides and adulticides on vector recruitment and mortality, the mosquito larva and adult compartments are also decreased. Seasonal forcing causes minor time variations to appear on top of these trends, demonstrating that oscillations do not need to be sustained even in the presence of periodic transmission. Dynamical systems analysis can be used to demonstrate that trajectories are limited and non-negative.

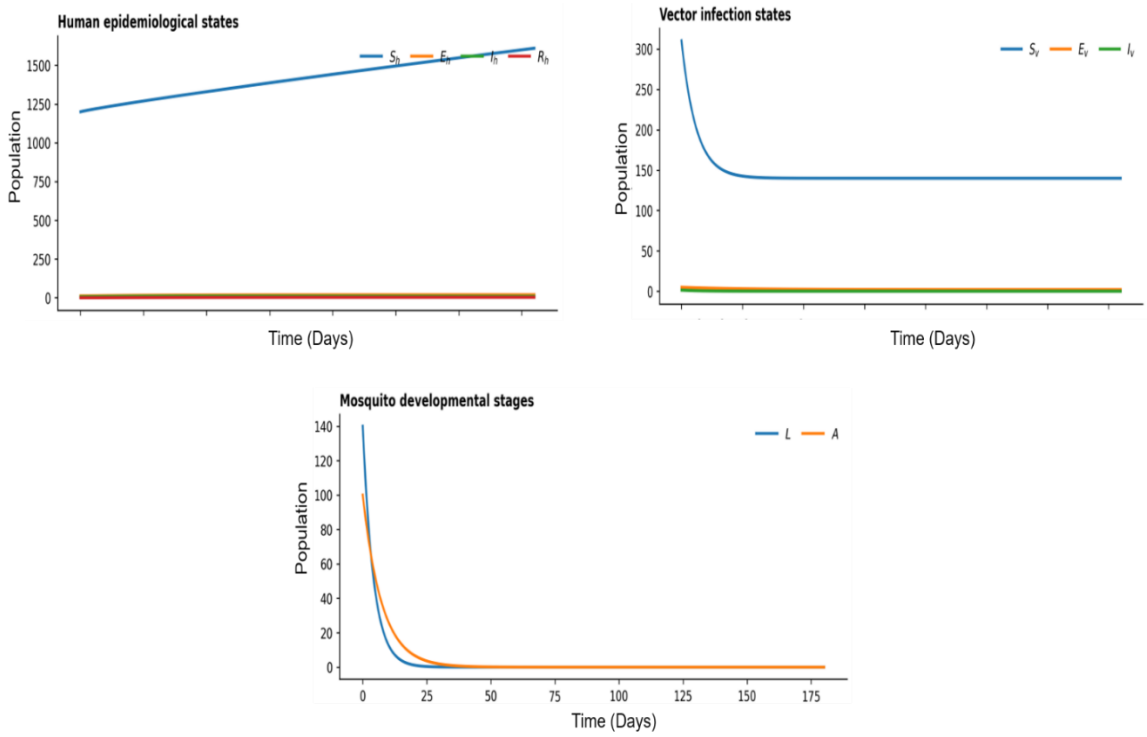


Figure 4: Nine Compartment Trajectories with Public Health Measures Integrated with Seasonal Forcing, the Graphs Categorize the States Based on Developmental Stages, Mosquito Infection and Human Epidemics

5.3 Phase Portrait Analysis of Disease Free Equilibrium

Table 5 shows that the initial conditions were intentionally changed in the phase-plane analysis so that the stability features could be examined using varying infection levels. All of the following variables were placed within the biologically possible region, susceptibles, exposed, infected, recovered, larvae, and adults. It was possible to identify discrepancies based just on the initial conditions because the same parameter values were utilized to evaluate the disease-free convergence.

Table 5: Numerical Assessments for Convergence in Phase Plane and Evaluation of Intervention Thresholds

Anslysis of Parameters	Analysis	u_1	u_2	u_3	R_0	$I_h(0)$	$I_v(0)$
Fixed Baseline Parameters	Disease-free IC	0.40	0.65	0.65	0.920	2	0.5
b_1 =2.8, c =0.00008	Disease-free IC	0.40	0.65	0.65	0.920	8	2
β_1 =1.8,	Disease-free IC	0.40	0.65	0.65	0.920	20	5
β_2 =0.85	Disease-free IC	0.40	0.65	0.65	0.920	35	10
α_v =0.032	Disease-free IC	0.40	0.65	0.65	0.920	60	18
α_h =0.007	Intervention scenario	0.60	0.75	0.65	0.751	40	15
r_0 =0.60, ε =0.22	Intervention scenario	0.50	0.65	0.55	1.023	40	15
μ_v0.075, δ_v =0.00012	Intervention scenario	0.40	0.55	0.45	1.408	40	15
γ_h =0.0011, μ_h =0.00030	Intervention scenario	0.20	0.35	0.25	2.952	40	15

Figure 5 uses a phase plane map of infected vectors and humans to evaluate the disease-free regime. The dependency on initial burden is assessed using five sets of initial infected states. Trajectories differ depending on the ratio of initial infection between humans and vectors, but they converge to the same asymptotic area near the infected free state. Directional convergence in both directions indicates a decrease in the infection subsystem's amplitude. Since the reproduction number for the aforementioned parametric configuration is smaller than one, the numerical solution satisfies the stability criterion as the next generation matrix formulation predicts. Most significantly, there is no cycle, outward spiral, or trajectory that diverges to infinity in the phase portrait. This implies that rather of continuing to amplify periodically, the process converges. Therefore, in the physiologically possible state space, the new data set provides independent numerical validation of disease eradication. The asymptotic behavior is the same under various initial conditions.

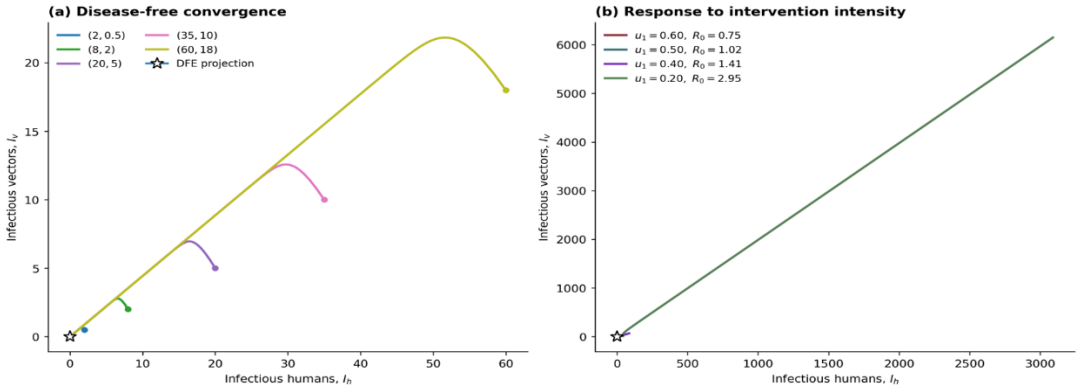


Figure 5: Convergence from Different Initial Infection States in a Disease-Free Setting to Phase-Plane of Infected Humans and Vectors

5.4 Parameter Sensitivity Analysis of Tansmission and Growth Dynamics Population

The transmission-sensitivity analysis dataset was produced by methodically sweeping each parameter about its corresponding baseline value one at a time. The model provided the metrics for infection load and reproduction number for each sweep. The mathematical impact of each cross-species transmission pathway can be ascertained using this method.

Table 6: Individual Sensitivity Numerical Values for the Two Rates of Cross-Species Transmission

Sweep	Coefficient	R_0	Peak I_h	Cumulative I_h	Cumulative I_v
β_1	1.200	0.776	18.32	1859.9	24.5
	1.400	0.839	19.59	1936.5	25.3
	1.600	0.897	20.91	2014.6	26.0
	1.800	0.951	22.27	2094.4	26.8
	2.000	1.002	23.67	2175.7	27.7
	2.200	1.051	25.12	2258.6	28.5
	2.400	1.098	26.61	2343.1	29.3
β_2	0.550	0.765	19.32	1946.9	17.9
	0.650	0.832	20.28	1995.5	20.8
	0.750	0.893	21.27	2044.6	23.8
	0.850	0.951	22.27	2094.4	26.8
	0.950	1.005	23.29	2144.7	30.0
	1.050	1.057	24.33	2195.6	33.3
	1.150	1.106	25.39	2247.0	36.7

Figure 6 provides an illustration of this, showing how the two cross-species transmission rates respond to systematic perturbations. When the level of transmission increases, distinct sweeps indicate increases in the reproduction threshold. At low levels, the maximum number of infectious individuals is approximately 18 – 19, at high levels, it is 26. As the overall burden of infectious vectors rises, so does the overall burden of infectious humans. These patterns imply that within the non-linear feedback system between the host and vector populations, the transmission coefficients function as high leverage parameters. The response trend has no abrupt discontinuities and is smooth across the range under consideration. In terms of sensitivity analysis, the response's direction corresponds with the transmission parameter's positive normalized influence.

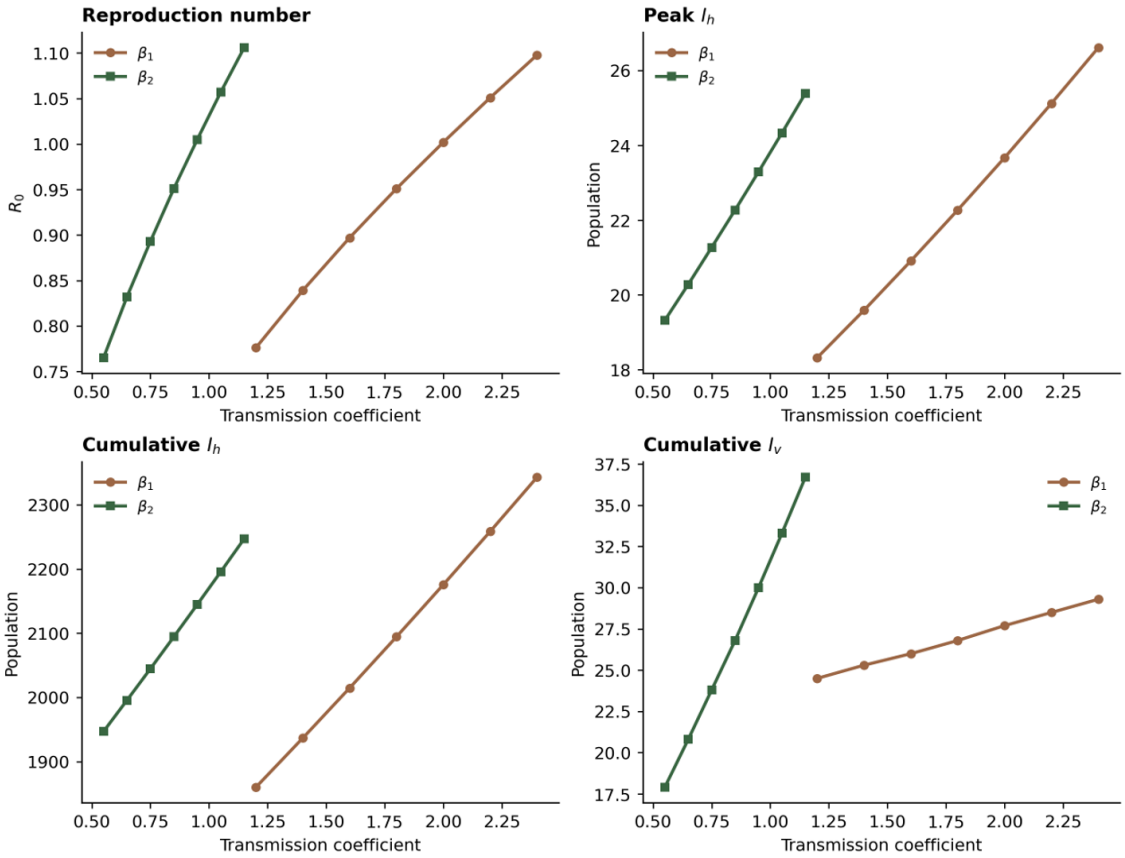


Figure 6: Sensitivity Examination of the Disease Burden and Reproduction Number to Rates of Vector-to-Host and Host-to-Vector Transmission

The numerical experiment examines vector development time and human recovery time, two biologically significant time-scale characteristics. While every other parameter had a baseline value, each parameter was evaluated over five distinct levels. The data was summarized using peak infection numbers, overall infection numbers, and recovered persons, if relevant.

Table 7: Response Parameter Numerical Assessments for Vector Evolution and Human Recuperation

Parameter	Value	Peak I_h	Cumulative I_h	Secondary Response
α_v	0.020	19.02	1925.2	1.50
	0.026	20.63	2009.7	1.50
	0.032	22.27	2094.4	1.50
	0.038	23.93	2179.2	1.50
	0.044	25.62	2264.1	1.50
γ_h	0.0007	23.19	2147.8	1.48
	0.0010	22.50	2107.6	2.07
	0.0013	21.83	2068.3	2.64
	0.0016	21.18	2030.1	3.19
	0.0019	20.56	1992.9	3.72

Figure 7(a) simulates five different parameter values to examine the effect of vector development rate on epidemic performance. An growing infectious-human peak value, spanning from 19.0 to 25.6, results from increasing the rate of development from 0.020 to 0.044. In terms of mathematics, this is because the rate of development modifies the vector subsystem's time scale, which in turn modifies the feedback effect on the human subsystem. Figure 7(b) evaluates the impact of the human recovery rate as a controlling factor in the dynamics of infection. The maximum number of infectious persons decreases from 23.2 to 20.6 individuals, and the infectious load decreases over the investigated range of recovery rates, from 0.0007 to 0.0019. Nonetheless, the maximum number of humans who have recovered increases in tandem, indicating the transition of individuals from the infectious condition to recovery. From the perspective of dynamical systems, the decay rate of the infected subsystem is impacted by an increase in the recovery rate.

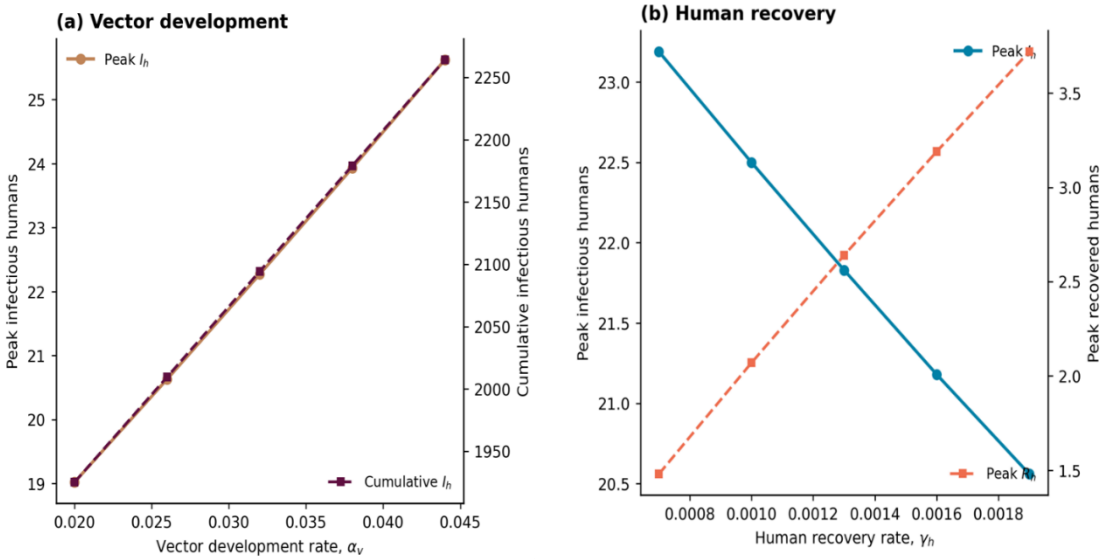


Figure 7: Response Profiles to Parameters from the Dynamical System, (a) Influence of Vector Development Rate on Infection Levels, (b) Influence of Human Recovery Rate on Infection and Recovery

6. Discussion

Temporal variability and the characteristics characterizing the host-vector system control the transmission dynamics via vectors. The periodically forced compartment model is more suitable if the vectors' transmission or demography are affected by environmental changes. This is because the vector field becomes temporally variable and the analysis of static equilibria should be distinct from that of dynamic periodic behavior. While Ibrahim and Dénes (2021) have established the non-autonomous Zika model with the reproduction threshold coupled to periodic infection operator, Ting-Ting et al. (2020) have demonstrated that seasonality may affect the threshold features if the aquatic stage of mosquitoes is explicitly incorporated. Nipa et al. (2021) shown that in seasonally fluctuating vector species, population and environmental fluctuation could affect the likelihood of an outbreak. According to a study by Khong et al. (2023), the significance of seasonality for the disease's persistence varies depending on the stage of the pathogen-vector interaction's life cycle that undergoes periodic alterations.

The transmission between subsystems with distinct time scales distinguishes between the epidemiological conditions of the human host population and those of the vector population. Maturation, recruitment, mortality, infection, and vector infection can all change at varying rates. According to Feng et al. (2021), the mathematical formulation of malaria vector models may be impacted by certain assumptions regarding residence-time distributions. This can be used to formulate ordinary differential equations with exposed and infected compartment transition rates. Further evidence that host-vector transmission may depend on mobility and linkages comes from structured spatial extensions. While Gao and Yuan (2024) demonstrated how host occupancy and vector mobility could alter persistence features in heterogeneous contexts, Zhao and Liu (2022) connected reproduction numbers, global stability, and control in network models. Therefore, formulations in compartmental models should be considered structured models where the translation of biological heterogeneities into the state space determines the qualitative dynamics.

The exact moment of the controls' introduction into the transmission operator is taken into account while modeling control mathematically. While controlling larvae and adult vectors has an impact on infectious vector density and demographics, controlling host exposure is accomplished through host protection. Dianavinnarasi et al. (2021) emphasized the significance of time and development structures in control evaluation by integrating vector control into age structure with delay along with stability analysis. The study by Li et al. (2023) considers several mosquito controllers in both spatial and impulsive situations and demonstrates how the time of the intervention and the variety of the environment might affect the intervention design. We can regard control parameters as operators on the transmission or demographic process due to these mathematical models.

The mathematical approach for examining parameter alterations in a non-linear host-vector system is provided by sensitivity analysis. It is more pertinent to examine sensitivity in relation to the interaction of the structure rather than as a ranking of parameters since local perturbations might spread through the feedback mechanism between the infected host and the vector (Mushtaq et al., 2024). Without implying that numerical

data are genuinely empirical observations, perturbation analysis utilizing a base configuration can determine monotonicity, threshold nearness, and timeframes. Sensitivity analysis can be used to determine how biological parameter uncertainty affects a system's qualitative behavior in conjunction with equilibrium and phase space analyzes. In contemporary vector-borne disease models, threshold analysis, structured state space, forcing, and control-dependent dynamics are widely recognized as related quantitative biology concepts.

7. Conclusion

In regard to seasonality, mosquito biology, and intervention strategies, the paper develops a non-linear mathematical model framework for vector-borne disease transmission as a dynamic interaction between human hosts and vectors. The framework makes it easier to investigate feasible sets and analyze equilibrium, threshold parameters, and stability from a state space perspective while preserving the biological structure of human infection classes and vector life cycle stages. While the Jacobian and Lyapunov approaches provide different insights into equilibria, the next generation approach offers the threshold parameter for infection invasion. The transmission structure and the values of epidemic state variables can be systematically evaluated in relation to parameter alterations thanks to the sensitivity framework. By altering the transmission dynamics rather than treating them as separate processes, the composite control method and the efficiency of interventions framework enable the integration of different intervention tactics into a cohesive framework. Seasonal forcing expands the analysis framework beyond the context of autonomous equilibrium and introduces temporal dependency. The model provides a framework for integrating environmental variability, vector biology, intervention factors, and epidemiology into a unified system. Future generalizations of spatial heterogeneity, stochastic processes, time delays, and optimum control are all possible with this model approach.

8. References

Akanni, J. O. (2026). Mathematical model of yellow fever transmission dynamics with human hosts and incorporating seasonally varying mosquito recruitment. *The European Physical Journal Plus*, *141*(1), 1.

Alalhareth, F. K., Atta, U., Ali, A. H., Ahmad, A., & Alharbi, M. H. (2023). Analysis of leptospirosis transmission dynamics with environmental effects and bifurcation using fractional-order derivative. *Alexandria Engineering Journal*, *80*, 372-382.

Bera, S., Khajanchi, S., & Roy, T. K. (2023). Stability analysis of fuzzy HTLV-I infection model: a dynamic approach. *Journal of Applied Mathematics & Computing*, *69*(1), 171-199.

Cui, M., Li, F., & Geng, F. (2025). Global Dynamics of Mosquito Population Model With Seasonality and Spatial Heterogeneity. *Mathematical Methods in the Applied Sciences*, *48*(12), 11850-11862.

Dhandapani, S., Venkatasubramaniam, B., Alsulami, I. M., Alsulami, A., Soundararajan, H., & Lingeshwaran, S. (2026). A dynamical approach for a fractional-order SEIL epidemic model embedding time delay. *AIMS MATHEMATICS*, *11*(6), 15725-15744.

Dianavinnarasi, J., Raja, R., Alzabut, J., Niezabitowski, M., Selvam, G., & Bagdasar, O. (2021). An LMI Approach-Based Mathematical Model to Control Aedes aegypti Mosquitoes Population via Biological Control. *Mathematical Problems in Engineering*, *2021*(1), 5565949.

Erandi, K., Perera, S., & Mahasinghe, A. (2021). Analysis and forecast of dengue incidence in urban Colombo, Sri Lanka. *Theoretical Biology and Medical Modelling*, *18*(1), 3.

Feng, Z., Gurski, K., Prosper, O., Teboh-Ewungkem, M., & Grogan, M. (2021). A mosquito-borne disease model with non-exponentially distributed infection and treatment stages. *Journal of Dynamics and Differential Equations*, *33*(4), 1679-1709.

Fesce, E., Marini, G., Rosà, R., Lelli, D., Cerioli, M. P., Chiari, M., Farioli, M., & Ferrari, N. (2025). Are we doing our best to contain the spread of West Nile virus? Evaluating intervention efficacy through mathematical modelling. *Parasites & Vectors*, *18*(1), 499.

Gao, D., & Yuan, X. (2024). A hybrid Lagrangian–Eulerian model for vector-borne diseases: D. Gao, X. Yuan. *Journal of Mathematical Biology*, *89*(2), 16.

Ibrahim, M. A., & Dénes, A. (2021). Threshold Dynamics in a Model for Zika Virus Disease with Seasonality: MA Ibrahim, A. Dénes. *Bulletin of Mathematical Biology*, *83*(4), 27.

Jothika, S., & Radhakrishnan, M. (2025). Stability and Control of a Vector-Host Disease Model with Time Delay

and Saturated Treatment. *Malaysian Journal of Mathematical Sciences*, *19*(1).

Kamiya, T., Greischar, M. A., Wadhawan, K., Gilbert, B., Paaijmans, K., & Mideo, N. (2020). Temperature-dependent variation in the extrinsic incubation period elevates the risk of vector-borne disease emergence. *Epidemics*, *30*, 100382.

Khong, V. H., Carmona, P., & Gandon, S. (2023). Seasonality and the persistence of vector-borne pathogens. *Journal of The Royal Society Interface*, *20*(209), 20230470.

Kronfeld-Schor, N., Stevenson, T. J., Nickbakhsh, S., Schernhammer, E. S., Dopico, X. C., Dayan, T., Martinez, M., & Helm, B. (2021). Drivers of infectious disease seasonality: potential implications for COVID-19. *Journal of biological rhythms*, *36*(1), 35-54.

Li, Y., Zhao, H., & Wang, K. (2023). Dynamics of an impulsive reaction-diffusion mosquitoes model with multiple control measures. *Math. Biosci. Eng.*, *20*, 775-806.

Manisha, & Kumar, A. (2025). Modeling and Optimal Management of Control Policies for Vector-Borne Diseases: A Study of Cost-Effectiveness and Policy Impact. *Optimal Control Applications and Methods*, *46*(6), 2882-2915.

Momoh, A. A., Déthié, D., Isah, N. S., Dekera, W. J., Adewale, J. A., & Michael, A. I. (2024). Mathematical modeling and optimal control of a vector-borne rice yellow mottle virus disease: AA Momoh et al. *International Journal of Dynamics and Control*, *12*(2), 600-618.

Mubarak, S., Lone, P. N., & Hussain, A. (2026). Mathematical analysis of transmission dynamics in vector-borne diseases via a generalized SEIR model. *Discover Public Health*, *23*(1), 480.

Mushtaq, I., Sarwar, M. S., & Munzoor, I. (2024). A comprehensive review of Wolbachia-mediated mechanisms to control dengue virus transmission in Aedes aegypti through innate immune pathways. *Frontiers in Immunology*, *15*, 1434003.

Nipa, K. F., Jang, S. R.-J., & Allen, L. J. (2021). The effect of demographic and environmental variability on disease outbreak for a dengue model with a seasonally varying vector population. *Mathematical biosciences*, *331*, 108516.

Padder, A., Qureshi, S., Matouk, A., & Dehingia, K. (2025). Dynamical analysis of a vector-borne disease model with control function strategies. *Discover Applied Sciences*, *7*(9), 1031.

Padder, M., & Khan, A. (2022). Analysis of tumor-immune response model by differential transformation method. *Journal of Scientific Research*, *14*(1), 243-256.

Prasad, R., Sagar, S. K., Parveen, S., & Dohare, R. (2022). Mathematical modeling in perspective of vector-borne viral infections: a review. *Beni-Suef University Journal of Basic and Applied Sciences*, *11*(1), 102.

Rivu, N. N. K., Kamrujjaman, M., & Iqbal, A. (2025). HIV/AIDS suppression in North america: intervention plans and Cost-Effectiveness of UNAIDS 90-90-90 and 95-95-95 targets. *Communications in Nonlinear Science and Numerical Simulation*, 109246.

Romero-Leiton, J. P., Laison, E. K., Alfaro, R., Parmley, E. J., Arino, J., Acharya, K. R., & Nasri, B. (2025). Exploring Zika's dynamics: A scoping review journey from epidemic to equations through mathematical modelling. *Infectious Disease Modelling*, *10*(2), 536-558.

Swei, A., Couper, L. I., Coffey, L. L., Kapan, D., & Bennett, S. (2020). Patterns, drivers, and challenges of vector-borne disease emergence. *Vector-Borne and Zoonotic Diseases*, *20*(3), 159-170.

Ting-Ting, Z., Lin-Fei, N., Zhidong, T., & Yantao, L. (2020). Modeling seasonal variation for mosquito-borne disease in the tropical monsoon environment. *Advances in Continuous and Discrete Models*, *2020*(1).

Ullah, S., Khashan, M. M., Shah, K., & Abdeljawad, T. (2026). Novel tick-borne encephalitis transmission dynamics: A model-based strategy for epidemic control. *Networks & Heterogeneous Media*, *21*(2), 1.

Yan, J., Hu, B., Guan, Z.-H., & Zhang, D.-X. (2025). On controllability of fractional-order impulsive and switching systems with time delay. *Applied Mathematics and Computation*, *497*, 129357.

Zhao, R., & Liu, Q. (2022). Dynamical behavior and optimal control of a vector-borne diseases model on bipartite networks. *Applied Mathematical Modelling*, *102*, 540-563.